

## Arnold diffusion in many weakly coupled mappings

Allan J. Lichtenberg and Anish M. Aswani

*Department of Electrical Engineering and Computer Sciences and the Electronics Research Laboratory, University of California, Berkeley, California 94720*

(Received 29 December 1997)

When standard maps are coupled together, particles diffuse along stochastic layers by the process of Arnold diffusion. For fixed nonlinearity parameter  $K$  and fixed coupling  $\mu$ , the diffusion increases with the number of maps,  $N$ , and the number of phases in each coupling term,  $m$ , where  $2 \leq m \leq N$ . For relatively large  $K$ , as  $N$  is increased, the diffusion rate increases as  $N^{1/2}$ , the length of the diagonal in the action space. For smaller  $K$  there is a cancellation of the  $N^{1/2}$  dependence. As  $m$  is increased, the diffusion rate increases as the phase of the coupling term for a particular map becomes less correlated with the phase of the map itself, but levels off for large  $m$ . For  $K=0.8$ , when the effect of  $N$  is removed by dividing the diffusion distance  $\Delta I_{\text{rms}}$  by  $N^{1/2}$ , curves of universal global diffusion  $\Delta I_{\text{rms}}$  versus  $m$  are found, for  $m \neq N$  and for  $m = N$ , with the latter lying somewhat below the former. For local Arnold diffusion, the increase in  $\Delta I_{\text{rms}}$  for a particular  $m$  depends strongly on the stochasticity parameter  $K$ , while the  $K$  dependence is much weaker for global diffusion for  $m \geq 3$ . An analytic calculation of the  $K$  dependence for the two cases indicates the reason for the difference. The analytic calculation has been compared to numerics over a range of  $m$  values for  $K=0.8, 0.4$ , and  $0.3$  in giving reasonable agreement. A weak global scaling of  $\Delta I_{\text{rms}} \propto K^{0.25}$  is found analytically and is qualitatively explained by the scaling of the dominant terms in the analytic expression. [S1063-651X(98)07405-4]

PACS number(s): 05.45.+b, 05.60.+w

### I. INTRODUCTION

In nonintegrable Hamiltonian systems of more than two degrees of freedom, Kolmogorov-Arnold-Moser (KAM) curves cannot isolate the stochastic layers that lie along the separatrices of system resonances. Stochastic layers lie along an interconnected web of resonances such that initial conditions in any part of the web can ultimately diffuse to all parts of it. The process, first proved to exist by Arnold [1] and now known as Arnold diffusion, has been studied in a variety of problems.

If three resonances can be locally isolated to be of dominant importance, then a method exists for calculating the rate of diffusion along a local resonance layer, known as the three-resonance model [2] or the stochastic pump model [3,4]. The model has been used to analytically calculate the local diffusion rate for coupled maps [2-4], and for coupled standard maps in particular [5,6], with good agreement obtained with numerical results for the case of two coupled maps. The three-resonance model predicts  $D = (\Delta I)^2/t \propto e^{-A/\epsilon^{1/2}}$  where  $\epsilon$  is the perturbation parameter and  $A \approx 1$ .

If many resonance layers overlap then the three-resonance model is not adequate to describe the diffusion, which can be much larger than that calculated using a three-resonance model. An upper bound on the diffusion rate has been obtained by Nekhoroshev [7] of the form  $D \propto e^{-A/\epsilon^\gamma}$  ( $A \approx 1$ ) where, for the number of degrees of freedom  $L$ , the optimal value of  $\gamma$  has been shown to be  $\gamma \approx L^{-1}$  [8,9]. If  $L$  is large it is clear that such an exponentially small diffusion could only hold for very small  $\epsilon$ , otherwise the exponential factor would be essentially unity. It has been estimated that  $\epsilon < \epsilon_L \sim (\sigma_0^2/L)^{2L^2}$ , where  $\sigma_0$  is the rate of decrease of Fourier coefficients of an analytic perturbation [9]. For  $L$  large this limits  $\epsilon$  to very small values. Also, an upper bound is related

to the fastest local diffusion, while an average global diffusion is controlled by the portions of the phase space where the diffusion is slowest.

In a model problem in which many resonances overlap, for  $L=3$ , Chirikov, Ford, and Vivaldi [10] numerically investigated the scaling of the diffusion with  $\epsilon$ , finding that it agreed with the upper bound scaling for  $\epsilon$  small, while it followed the three-resonance model,  $\gamma = \frac{1}{2}$ , for larger  $\epsilon$ . However, the important  $L$  dependence was not investigated.

To investigate global diffusion it is useful to employ a system that has uniform properties in a coarse-grained sense. The standard map, described by the equations

$$I_{n+1} = I_n + K \sin \theta_n,$$

$$\theta_{n+1} = \theta_n + I_{n+1}, \quad \text{mod } 2\pi$$

where  $I$  is the action and  $\theta$  is the phase, has this important property as it is  $2\pi$  periodic in both angle and action. The well known phase space, as shown in Fig. 1 for  $K=0.8$ , consists of regions of stochasticity (area filling trajectories) surrounding island chains of rational frequency. The regions of stochasticity are separated by regular motion on phase-spanning KAM curves. The largest region of stochasticity (thick dark region) we refer to as the "primary stochastic region," and the thinner regions around smaller islands are "secondary stochastic regions." The KAM curves consist of two types, librational motion about fixed points (closed curves on the phase plane) and rotational motion (open curves spanning  $2\pi$  in the phase  $\theta$ ). For  $K \geq 0.9716 \dots$  the final rotational KAM curve is destroyed, such that global diffusion in a coupled set of mappings is across resonances rather than Arnold diffusion along resources.

Konishi and Kaneko [11] studied global diffusion in a set of coupled mappings of the form

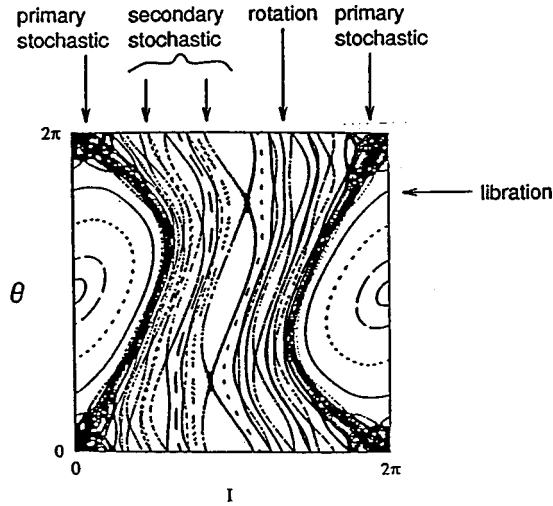


FIG. 1. The standard map for  $K=0.8$ , with a number of initial conditions used to explore both regular and stochastic orbits.

$$p_i(t+1) = p_i(t) + \frac{K}{2\pi} (\sin\{2\pi[x_{i+1}(t) - x_i(t)]\} - \sin\{2\pi[x_i(t) - x_{i-1}(t)]\}),$$

$$x_i(t+1) = x_i(t) + p_i(t+1), \quad \text{mod } 1, \quad i = 1, 2, \dots, N \quad (1a)$$

in which nearest neighbors are coupled, and

$$p_i(t+1) = p_i(t) + \frac{K}{2\pi\sqrt{N-1}} \sum_{j=1}^K \sin\{2\pi[x_j(t) - x_i(t)]\},$$

$$x_i(t+1) = x_i(t) + p_i(t+1), \quad (1b)$$

for which there is all-to-all global coupling. They investigated the diffusion for  $0.2 \leq K \leq 1$ , over a range of  $N$  values. For nearest neighbor coupling and  $N > 3$  the diffusion coefficient  $D$  fitted an exponential with the power of  $\epsilon \equiv K$  given by  $\gamma \approx 0.45$  and independent of  $N$ . This is quite different from the estimates obtained from the rigorous upper bounds, and is, in fact, close to  $\gamma = 0.5$  predicted from a three-resonance model. For global coupling an exponential form did not fit well, but for  $N = 4, 5$ , and  $6$  they found for  $K < 1$  that  $D \propto K^\gamma$  with  $\gamma \approx 5$ .

Using a general analysis similar to that employed to obtain an upper bound to the diffusion, but applied to larger values of  $\epsilon$ , Chirikov and Vecheslavov [12] have estimated that the rate of global diffusion for  $L$  sufficiently large and  $\epsilon$  not too small behaves as a power law in  $\epsilon$ ,  $D \propto \epsilon^\eta$ , with  $\eta \approx 6.5$ , and is independent of  $L$ . The value of  $\eta$  can be adjusted by a fitting parameter, which was used to fit the data in [11] for the case of nearest neighbor coupling. However, as described above, the exponential fitting, which agrees with the three-resonance model, also fit quite well over the parameter range.

The forms of the mapping studied by Konishi and Kaneko [11] do not distinguish how many resonances are driving the diffusion, and do not distinguish the strength of the coupling from the nonlinearity. We adopted an alternate procedure of

linking simple standard maps together through a weak coupling term [5,6] (see also [13]):

$$I_{n+1}^1 = I_n^1 + K^1 \sin \theta_n^1 + \mu \sin(\theta_n^1 + \dots + \theta_n^m),$$

$$\theta_{n+1}^1 = \theta_n^1 + I_{n+1}^1, \quad \text{mod } 2\pi,$$

$$\vdots$$

$$I_{n+1}^N = I_n^N + K^N \sin \theta_n^N + \mu \sin(\theta_n^N + \dots + \theta_n^{m-1}),$$

$$\theta_{n+1}^N = \theta_n^N + I_{n+1}^N, \quad \text{mod } 2\pi,$$

where a total of  $N$  maps are coupled together in groups of  $m$ , with  $2 \leq m \leq N$ ; each map is coupled to itself and the next  $m-1$  maps in cyclical order. Note that this system has  $L = N+1$  degrees of freedom (also called  $N + \frac{1}{2}$  degrees of freedom, since the additional freedom is the time). We leave the structure of the individual maps nearly unchanged by making the coupling strength  $\mu$  small, and control the number of interacting resonances through the number of coupling phases. The nonlinearity parameters  $K^i$ ,  $1 \leq i \leq N$ , can also be varied independently of the coupling. The mapping equations (2) are volume preserving and are also reversible, but do not have a complete symplectic form unless  $m = N$ .

In previous work [6] the mappings were numerically integrated, for a large set of initial conditions chosen to be in the stochastic phase space of the individual maps, with  $K = 0.8$ , and for various values of  $m$  and  $N$ . The action  $I$  was allowed to range over all values, to determine the action diffusion  $\Delta I_{\text{rms}}$ . The values of  $K$  and  $\mu$  were chosen to be sufficiently large that the diffusion rate could be determined in a reasonable time (typically  $2^{21}$  iterations per mapping for each initial condition), while  $\mu$  was chosen sufficiently small so as not to greatly perturb the phase space of the individual maps. When the effect of  $N$  was removed by dividing the diffusion distance  $\Delta I_{\text{rms}}$  by  $N^{1/2}$ , a universal global diffusion  $\Delta I_{\text{rms}}$  vs  $m$  was found, for  $m \neq N$ . For  $m = N$ , for which the mapping has a symplectic structure, a somewhat different  $\Delta I_{\text{rms}}$  vs  $m$  was found. The difference between these two results was tentatively interpreted, without proof, as the difference between mappings with and without a symplectic structure. One of the objectives of the present paper is to test this interpretation by constructing mappings with  $m \neq N$  but having a symplectic structure, and compare the diffusion to that of the previously studied mappings.

The local rate of Arnold diffusion can be calculated, using a generalization of the three-resonance model [2,4]. This was done in previous work [5,6] obtaining good agreement with numerical diffusion over a limited range of  $m$  and  $K$ . A formula for global diffusion was obtained, using a generalization of phase space arguments that had been developed to treat a simpler problem [14]. Due to the complexity of the formula for large  $m$ , the comparisons with numerical results were only obtained for  $m = 2$  and  $3$ , obtaining reasonable (but not close) agreement for the only numerical perturbation strength considered, that of  $K = 0.8$ . In this paper we extend these results to a wide range of  $m$  values and to somewhat smaller  $K$  values that are still accessible, numerically. We

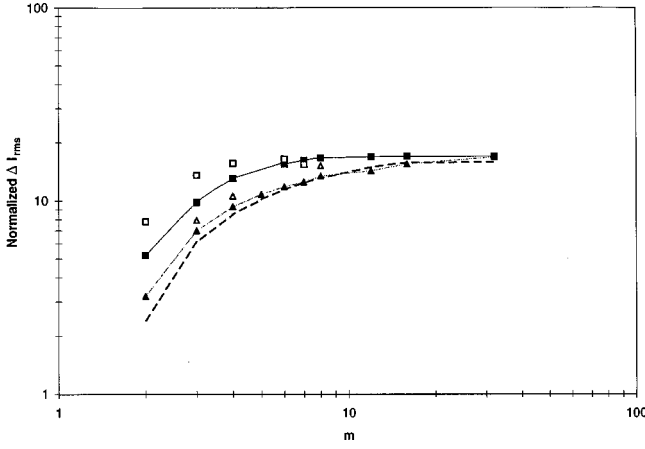


FIG. 2. Global  $\Delta I_{\text{rms}}$  vs  $m$ , normalized by dividing by  $N^{1/2}$ , for  $K=0.8$ ,  $\mu=0.01$ , and  $n=2^{21}$  mapping iterations. Solid squares and solid triangles are previous results for  $m \neq N$  and  $m=N$ , respectively. Open squares and open triangles are new results with  $m \neq N$  and  $m=N$ , respectively. Heavy dashed curve is theory.

also explore the scaling of the diffusion, analytically, over a wide range of  $K$  values to compare with other results [11,12].

## II. SYMPLECTIC MAPPING

A symplectic mapping can be derived from a generating function

$$\tilde{F} = \sum_{i=1}^N \left[ \bar{I}_i \theta_i + K_i \cos \theta_i + \frac{\mu}{\sqrt{m}} \cos \left( \sum_{j=1}^m \theta_{\{i+j-1\}} \right) \right], \quad (3)$$

where  $\{\}$  denote the cyclic coordinates if  $i+j-1 > N$ . For example, in place of Eq. (7), for  $m=2$  and  $n=3$ , the action transformations are

$$\begin{aligned} \bar{I}_1 &= I_1 + K_1 \sin \theta_1 + \frac{\mu}{\sqrt{2}} \sin(\theta_1 + \theta_3) + \frac{\mu}{\sqrt{2}} \sin(\theta_1 + \theta_2), \\ \bar{I}_2 &= I_2 + K_2 \sin \theta_2 + \frac{\mu}{\sqrt{2}} \sin(\theta_2 + \theta_3) + \frac{\mu}{\sqrt{2}} \sin(\theta_2 + \theta_1), \\ \bar{I}_3 &= I_3 + K_3 \sin \theta_3 + \frac{\mu}{\sqrt{2}} \sin(\theta_3 + \theta_1) + \frac{\mu}{\sqrt{2}} \sin(\theta_3 + \theta_2), \end{aligned} \quad (4)$$

with the accompanying phase transformations as in Eq. (2). As in previous work, we first consider  $K_1=K_2 \cdots =K_N=0.8$  and  $\mu=0.01$ . There are 128 initial conditions, in this and all subsequent calculations. We obtain the results given in Fig. 2, which are compared with the previous numerical results in [6], Fig. 11. All results are normalized by the number of initial conditions and the number of mappings.

$$\Delta I_{\text{rms}}^2(n) = \sum_{i=1}^M [I_i(n) - I_i(0)]^2 / NM^2,$$

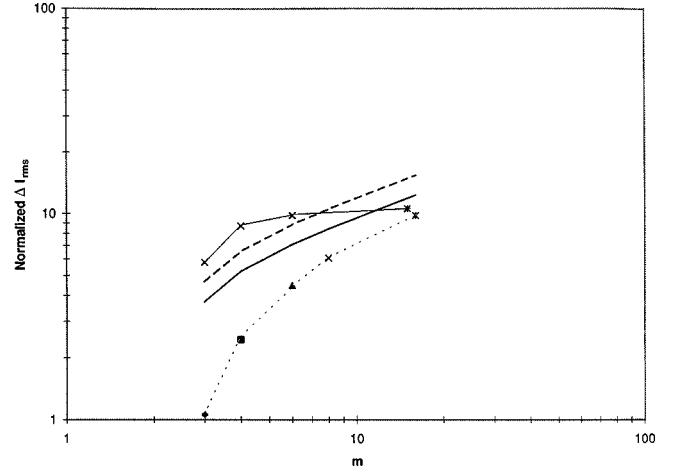


FIG. 3. Global  $\Delta I_{\text{rms}}$  vs  $m$ , for  $K=0.4$ ,  $\mu=0.005$ , and  $n=2^{21}$  normalized by dividing by  $N^{1/2}$  and multiplying by  $0.01/0.005$  in order to compare with  $K=0.8$  results. Crosses for  $N=8$ ; triangles, squares, and diamonds for  $N=6, 4$ , and  $3$ , respectively. Asterisk is for  $N=16$ . Light solid line is through cases with  $m \neq N$  and light dotted line is through cases with  $m=N$ . Heavy solid and dashed curves are theoretical (see text).

where  $M$  is the number of initial conditions. We see that the new results for the not fully coupled but symplectic maps lie above the results for fully coupled maps and close to the results for the nonsymplectic maps. A theoretical curve (heavy dashed line) is also shown and will be discussed in the following section.

Various explanations for the difference between the symplectic mapping, as in Eq. (3), and the fully coupled case can be postulated. For the symplectic mapping we have normalized each coupling term, relative to the coupling terms of the nonsymplectic map by the square root of the number of coupling terms. This normalization implies that the coupling terms are independent over long time averages. The results indicate that the normalization is approximately correct but small correlations may still exist, accounting for the difference between the results. Another explanation is that there is some additional constraint due to the added symmetry of fully coupled systems.

In Fig. 3, the numerical results are given for  $K=0.4$  with  $\mu=0.005$ . A smaller  $\mu$  is used in order to reduce the effect of the perturbation term on the single map topology. The results are normalized to the value of  $\mu$  in Fig. 2 by multiplying  $\Delta I_{\text{rms}}$  by  $(0.01/0.005)$ , so that the two graphs can be directly compared. The results are also normalized by  $N^{1/2}$  but this normalization is seen to be not as good as in the  $K=0.8$  case. Theoretical curves corresponding to this case are also shown. These results will be discussed further in the next section.

Numerical results for smaller values of  $K$  are very hard to obtain, requiring very long runs before the diffusion emerges from the initial oscillations. For example, such a run for  $K=0.3$ ,  $\mu=0.005$ ,  $N=8$ , and  $m=4$  is shown in Fig. 4 for  $n=2^{24}$  iterations. We note that it took the full  $2^{24}$  iterations for the  $\Delta I_{\text{rms}} \propto n^{1/2}$  proportionality to be marginally established. In Fig. 5 numerical results are given for a limited number of  $m$  values, together with the theoretical curves, to be discussed in the next section.

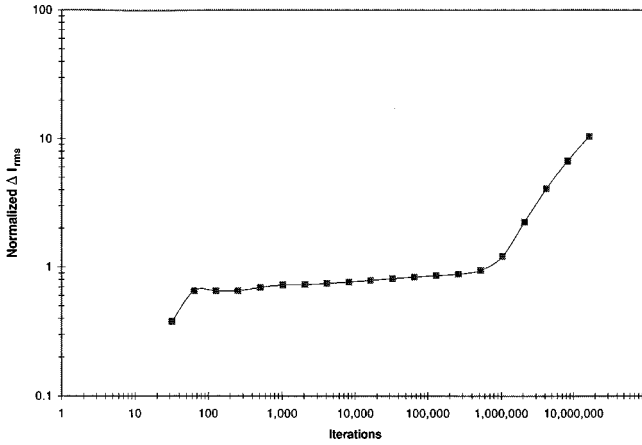


FIG. 4. Global  $\Delta I_{\text{rms}}$  vs  $n$  for  $K=0.3$ ,  $\mu=0.005$ ,  $N=8$ , and  $m=4$ , and  $n=2^{24}$ . Normalization as in Fig. 3.

We note that for  $m > 3$  but  $m < N$ ,  $\Delta I_{\text{rms}}$  is nearly independent of  $m$  for any  $K$ . This is consistent with the results for the globally coupled case in [11] for which the diffusion is nearly independent of the number of coupled maps  $N$ . It is also consistent with the theoretical results in [12]. However, for the strongly nonlinear case  $K=0.8$ , there is an additional limitation to the diffusion which is that  $\Delta I_{\text{rms}}$  cannot exceed the value given by a purely stochastic drive. Thus if the coupling phase is randomized on each iteration, an approximate limit to the normalized  $\Delta I_{\text{rms}}$  is

$$\Delta I_{\text{rms}} \approx \mu n^{1/2},$$

which for  $\mu=0.01$  and  $n=2^{21}$  gives  $\Delta I_{\text{rms}}=14.5$ , just about at the level of open squares for  $4 \leq m \leq 7$ . The estimation is not very sharp, due to the assumption that the coupling terms are independent. The values of  $\Delta I_{\text{rms}}$  for  $K=0.4$  and  $0.3$  lie below this limit and are more convincing as a signal that the results are nearly independent of  $m$ .

### III. ANALYTIC CALCULATIONS

A method of analytically calculating the global diffusion was developed in the previous work [5,6]. The method in-

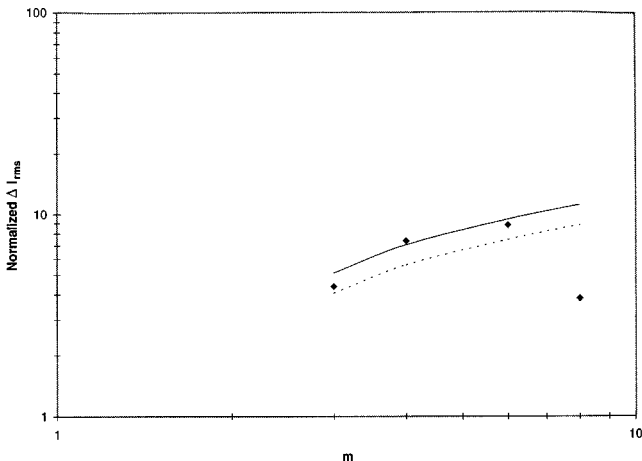


FIG. 5. Global  $\Delta I_{\text{rms}}$  vs  $m$  for  $K=0.3$ ,  $\mu=0.005$ ,  $N=8$ , and  $n=2^{25}$  normalized by dividing by  $N^{1/2}$ , multiplying by  $0.01/0.005$ , and by  $(2^{21}/2^{25})^{1/2}$  to compare with other  $K$ -value results. Solid and dashed curves are theory.

involved two stages: (1) a calculation of the local diffusion across phase-spanning rotation orbits at a given value of action; and (2) a phase space averaging procedure to determine the average rate of global diffusion for each map. We summarize the formulas, here, without presenting a complete discussion.

If there are  $m$  coupling phases in a single coupling term of which there are  $p$  driving phases,  $d=r+s$  rotation and secondary stochastic phases, and  $l$  libration phases ( $m=p+d+l$ ), the local diffusion coefficient along any of the  $d$  actions  $\mathbf{I}=(I_1, \dots, I_d)$  can be written in the form of a modified binomial expansion [6]

$$D_{pd}(\mathbf{I}) = \frac{\mu^2}{2K_j T} \sum_{i=1}^p \binom{p}{i-1} \left(\frac{\Delta t}{T}\right)^{p-i} \left(1 - \frac{\Delta t}{T}\right)^{i-1} \times \frac{1}{\pi} \int_{-\pi/2}^{\pi/2} \cos^{2(p-i)} \theta' d\theta' A_{\text{MA}}^2(p+1-i), \quad (5)$$

where  $(\Delta t/T) \approx K/2$ ,  $T=2\pi^2/K_j$ , and  $Q_d = \omega_d/K_j^{1/2}$ , with  $\omega_d = I_1 + I_2 + \dots + I_d \bmod 2\pi$  for  $0 < \omega_d < \pi$ , and  $\omega_d = 2\pi - [(I_1 + I_2 + \dots + I_d) \bmod 2\pi]$  otherwise.  $A_{\text{MA}}(k)$  is the peak value of the Melnikov-Arnold (MA) integral for  $k=p+1-i$  stochastic drives. We see that this coincides with the usual set of MA integrals as defined in [2,4],  $A_{\text{MA}}(k) = A_{2k}$ , where  $A_{2k}$  is determined by the recursion relation for MA integrals  $A_{\ell} = [2Q_0/(\ell-1)]A_{\ell-1} - A_{\ell-2}$ , with  $A_1 = 2\pi e^{\pi Q_0^2/\sinh \pi Q_0}$  and  $A_2 = 2Q_0 A_1$ . In previous work [6] the local diffusion, calculated from Eq. (5), was compared to numerical results for a specific value of  $I$ . This was done by taking all maps but one to be in their primary stochastic layers, but uncoupled from each other, but all coupled to one mapping through a single coupling term as

$$I_{n+1}^1 = I_n^1 + K \sin \theta_n^1 + \mu \sin(\theta_n^1 + \dots + \theta_n^m). \quad (6)$$

Taking values of  $K=0.2$  for all maps, and  $\mu=10^{-4}$  for the single coupling term, chosen to be sufficiently small that the diffusion remained local over  $n=2^{18}$  iterations, and  $I_i=2.35$ , chosen to be in a regular region, excellent agreement between the numerical value of  $\Delta I_{\text{rms}}$  and the value calculated from  $\Delta I_{\text{rms}} = [D_{pd}(\mathbf{I})n]^{1/2}$  was obtained ([6], Fig. 9), up to  $m=16$ . We have extended this comparison to  $m=32$  with continued excellent agreement between theory and numerics.

For calculating global diffusion we consider identical maps and take the coupling to the phase of the map being considered, and  $m-1$  other phases assumed to act identically over very long times. This is the ergodic assumption, which implies that all regions of the accessible phase space are explored over these long times with a probability that is proportional to the phase space areas. To apply the assumption to a non-steady-state global diffusion problem we use the approximation that the more accessible portion of the phase space, which fills on the time scale required to calculate the diffusion, is sufficiently close to the total accessible phase space that a reasonably accurate calculation can be made. The hypothesis of asymptotic ergodicity has been checked for a simpler two-dimensional (2D) mapping [14]. Following the reasoning in Ref. [5], we assume that in a

coupled map the primary stochastic region (which we will denote  $P$ ) can drive Arnold diffusion across rotational orbits ( $R$ ) and across the stochastic regions associated with the secondary resonances ( $S$ ). It can also drive diffusion across a librational region ( $L$ ), but this does not contribute to global diffusion because the motion averages to the location in action of the fixed point of a librational region. We determine the probabilities of a particle being in the various accessible regions of phase space, and the effect of the diffusion in each region.

Before considering the probabilities of the different types of phase space in which diffusion is taking place, we first define appropriate averages over the diffusing (driven) direction. If there is only one regular phase in the coupling term,  $d=r+s=1$ , then the average diffusion coefficient  $\bar{D}_{p1}$  for the diffusing action, say  $I$ , is obtained by averaging the reciprocal of  $D_{p1}(I)$  over  $I$ . Since the  $R$  and  $S$  regions are closely intermingled in action while  $D_{p1,R}$  varies slowly over these regions, and the secondary stochastic layers are generally thin, we approximate the reciprocal diffusion as

$$\frac{1}{\bar{D}_{p1}} = \frac{R}{R+S} \frac{1}{\pi} \int_{R+S} \frac{dI}{D_{p1,(R+S)}(I)}, \quad (7)$$

where we have eliminated the  $P$  and  $L$  regions from this average because the  $D_p$  for primary stochastic orbits is large and librational orbits only store particles. If there is more than one regular or secondary stochastic phase in the coupling term,  $d \geq 2$ , then these phases add to give a combined sum of actions  $I_d = \omega_d$ , as described previously. Since all values of action for the phases other than the diffusing phase are possible, an average is performed over these other actions,

$$D_{p2}(I) = \int D_{p2}(\mathbf{I}) d\mathbf{I}' \Big/ \int d\mathbf{I}', \quad (8)$$

where  $\mathbf{I}'$  is an integration over all of the  $I$ 's except the diffusing one, and the subscript  $p2$  indicates that  $d=r+s \geq 2$  in the coupling term. As discussed above, we assume that only actions in the  $R$  and  $S$  regions contribute, while the  $L$  actions are considered to oscillate about zero. To evaluate  $D_{p2}$ , we note that two or more regular phases appear as a sum in the coupling term; hence, they can be considered as a single regular phase in evaluating the MA integral. This has been confirmed numerically. Performing the integral in Eq. (7) over the allowed ranges of all actions  $\mathbf{I}'$  yields the result that  $D_{p2}(I) = \text{const}$ , independent of the diffusing (driven) action  $I$ . The final average of  $D_{p2}^{-1}$  as in Eq. (6) to yield  $\bar{D}_{p2}$  is then trivial.

Summing the various contributions, as in [6] we have

$$\begin{aligned} D_g(N, m) = & N \frac{R+S}{1-(R+L)^N} \sum_{p=1}^{m-1} \left\{ \bar{D}_{p2} \binom{m-1}{p} \right. \\ & \times P^p [(R+S+L)^{m-1-p} - L^{m-1-p}] \\ & \left. + \bar{D}_{p1} \binom{m-1}{p} P^p L^{m-1-p} \right\}, \quad (9) \end{aligned}$$

where, as previously,  $(R+S)$  is the fractional volume of the diffusing phase space,  $N$  is the number of maps in which diffusion can independently occur,  $P$  is the fractional volume of the phase space of the primary drive, and  $1-(R+L)^N$  is the fractional volume of the accessible phase space. For  $N$  large and relatively large  $K$ , the coefficient multiplying the summation in  $D_g$  is proportional to  $N$ , which explains  $\Delta I_{\text{rms}} \propto N^{1/2}$ , as found numerically for  $K=0.8$ .

For  $\mu \ll 1$  the various phase space areas can be found analytically [4]. From the first order Hamiltonian of the standard map

$$L \cong L_1 + L_2 = \left[ \frac{(2K)^{1/2}}{\pi^2} + \frac{K}{2\pi^2} \right] \int_0^\pi (1 - \cos \theta)^{1/2} d\theta, \quad (10)$$

which corresponds to the sum of the primary and two-iteration islands. From second order theory the primary stochastic layer has a phase space area given by

$$P = \frac{8}{\pi} \frac{(2\pi)^4}{K^{3/2}} \exp\left(-\frac{\pi^2}{K^{1/2}}\right) \quad (11)$$

and for reasonably small  $K$  ( $K \leq 0.4$ ) we can take  $S \approx 0$ . We then have  $R = 1 - L - P$  with all values normalized to the total phase space area. These values are quite good for  $\mu = 10^{-3}$ . In previous work, we investigated a particular example, that of  $K=0.8$  for all maps and  $\mu=0.01$ . For this larger value of  $\mu$  the stochastic phase spaces were found to be enlarged and were determined numerically [5]. The fractions of phase space in the various regions were found, for that example, to be  $P \approx 0.19$  primary stochastic,  $S \approx 0.30$  secondary stochastic,  $R = 0.11$  rotational, and  $L = 0.40$  librational. For our analytic comparisons with the numerical results of mapping iterations we use the numerical values for the special case of  $K=0.8$  and  $\mu=0.01$ , while for other cases, smaller  $\mu$  and smaller  $K$ , we use the analytic formulas, and modified analytic formulas, as described below.

In Fig. 2 we compare the numerical and analytic results for  $K=0.8$  and  $\mu=0.01$ , as described in Sec. II. As can be seen in the figure the numerical results lie above the theory (heavy dashed line) in the partially coupled case and are close for the fully coupled case.

In Fig. 3 the numerical and analytic results are compared for  $K=0.4$  and  $\mu=0.005$ . The results are renormalized to  $\mu=0.01$  so that direct comparison with  $K=0.8$  results can be made. For the analytic results, two approximations are made for the phase space areas, which were not measured directly. The theoretical values from Eqs. (10) and (11), which underestimate the areas give the lower curve (heavy solid line). The upper curve is obtained from the measured values at  $K=0.8$ , reduced proportionately by use of Eqs. (10) and (11) (heavy dashed line). The  $N$  normalization has also begun to be less accurate. The reason for this can be seen from the denominator factor in front of the summation in Eq. (9). Expanding  $1-(R+L)^N$  for small  $K$  ( $NP < 1$ ), we find the leading term gives

$$1 - (R+L)^N \cong NP$$

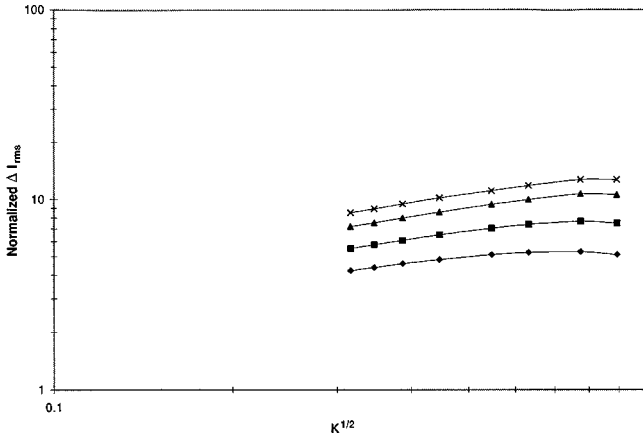


FIG. 6. Global  $\Delta I_{\text{rms}}$  vs  $K^{1/2}$  with  $m$  as a parameter, from theory. Diamonds, squares, triangles, and crosses are for  $m=3, 4, 6,$  and  $8,$  respectively.

and thus the  $N$  scaling of  $D_g$  cancels. For  $K=0.4$  this cancellation is beginning, and therefore the  $N$  normalization leaves numerical results at lower  $N$  somewhat above the higher  $N$  results.  $N=16$  is used for the theory and  $\Delta I_{\text{rms}}$  has been normalized by  $N$ .

In Fig. 5 the numerical and analytic results are compared for  $K=0.3$ ,  $\mu=0.005$ , and  $N=8$ . The results are normalized to  $\mu=0.01$  and by dividing by  $N^{1/2}$ . Since  $N=8$  for all  $m$ , in the figure, the  $N^{1/2}$  normalization is only for approximate comparison with the other  $K$  values, which also have this normalization. The two theory curves, as described above, are again shown.

To study the important scaling of  $\Delta I_{\text{rms}}$  with  $K$ , we use the analytic formulas, keeping in mind that we have not proven these scalings to accurately reflect the numerical results to small  $K$  values. In Fig. 6 the scaling is given with  $m$  as a parameter. We find a weak power-law scaling of

$$\Delta I_{\text{rms}} \propto K^\gamma,$$

with  $\gamma=0.25$ . The power law is essentially independent of the number of coupled degrees of freedom ( $m$ ) as in the other studies [11,12]. The calculations have not been extended to  $K < 0.08$  because subtraction of large nearly equal numbers led to increasing errors below this value. This precludes investigation of the upper bound scaling as in [7–9], but is in the proper regime for studying the power-law scaling [11,12].

To understand this weak theoretical scaling of  $\Delta I_{\text{rms}}$  with  $K$  for our system, we examine a dominant term in Eq. (8) of the type  $D_{p2}$ , given by Eq. (7). The important scaling derives from the Melnikov-Arnold integral. We examine the average of the lowest order integral  $A_2$ , which occurs in  $D_{12}$  which has the largest variation with  $K$ ,

$$\bar{A}_2 = \frac{1}{\pi} \int_0^\pi 4\pi \frac{I}{K^{1/2}} \frac{\exp[(\pi/2)(I/K^{1/2})]}{\sinh(\pi I/K^{1/2})} dI, \quad (12)$$

where the integral can be taken to extend over the entire phase space. At small  $I$  we expand  $\sinh(\pi I/K^{1/2})$  for small argument, to obtain an approximate relationship

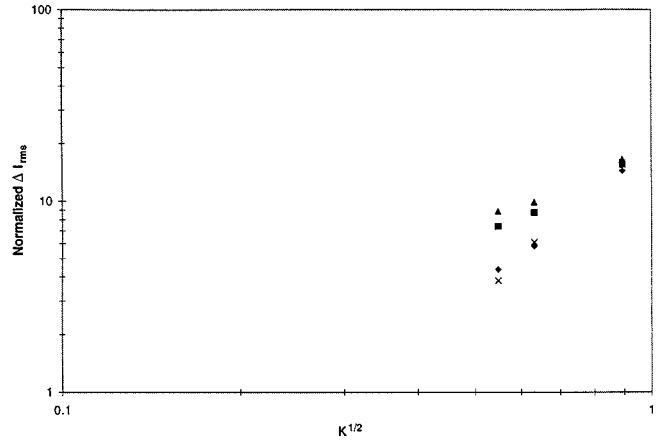


FIG. 7. Global  $\Delta I_{\text{rms}}$  vs  $K^{1/2}$  with  $m$  as a parameter, from numerical results,  $N=8$ . Diamonds, squares, triangles, and crosses are for  $m=3, 4, 6,$  and  $8,$  respectively.

$$\begin{aligned} \bar{A}_2 \sim & \frac{1}{\pi} \int_0^{2K^{1/2}/\pi} e^{(\pi/2)(I/K^{1/2})} dI \\ & + 4 \int_{2K^{1/2}/\pi}^\pi \frac{I}{K^{1/2}} e^{-(\pi/2)(I/K^{1/2})} dI, \end{aligned}$$

which can be evaluated to obtain, approximately,  $\bar{A}_2 \cong 1.1 K^{1/2}$ . Thus  $\bar{D}_{12} \propto K$  and if this is the dominant scaling,  $\Delta I_{\text{rms}} \propto \bar{D}_{12}^{1/2}$  such that

$$\Delta I_{\text{rms}} \propto K^{1/2}, \quad (13)$$

which is qualitatively similar to the value of  $\Delta I_{\text{rms}} \propto K^{0.25}$ , found from the complete calculation. The other  $D_{p2}$  terms, with  $p > 1$ , will be more weakly varying with  $K$ . Physically we can understand this result by noting that the theoretical value of  $\bar{A}_2$  is mainly determined by the near-resonant values of the regular phases where  $|\dot{\theta}_1 \pm \dot{\theta}_2| = O[K^{1/2}]$  for which the Melnikov-Arnold integral has a maximum value which is nearly independent of  $K$ . The fraction of the phase space for which this occurs is proportional to  $K^{1/2}$ , which accounts for the scaling in Eq. (13).

Although we cannot obtain a large range of  $K$  scaling, numerically, we obtain an approximate scaling over the three values of  $K=0.8, 0.4, 0.3$  for which we have numerical results, as shown in Fig. 7. For  $N=8$  we obtain the scaling for  $m=4$ ,  $\Delta I_{\text{rms}} \propto K^{0.8}$ , and for  $m=8$ ,  $\Delta I_{\text{rms}} \propto K^{1.4}$ . These numerical values are significantly above the theoretical values. An explanation of the higher numerical than theoretical proportionalities is that the times required to explore the phase space may be long compared to the numerical iteration time, such that the ergodic assumption is not satisfied. The numerical difference in  $K$  scaling between the  $N=8, m=4$  case and the  $N=8, m=8$  case may be another manifestation of the special properties of the fully coupled maps.

To compare our results with those discussed in the Introduction [11,12] we first note that we have separated the coupling parameter  $\mu$  from the nonlinearity parameter  $K$ . These are combined in [11,12]. Thus we obtain, theoretically,  $\Delta I_{\text{rms}} \propto \mu K^{1/4}$  or  $D \propto \mu^2 K^{1/2}$ . For  $\mu=K$  this corresponds to  $D \propto K^\gamma$  with  $\gamma=2.5$ . For the numerics, taking an approximate

average,  $\Delta I_{\text{rms}} \propto \mu K$ , we obtain  $\gamma \approx 4$ . Both of these values of  $\gamma$  are below the value of  $\gamma = 4.8$  found in [11], with the theoretical result significantly below either numerical result. We note that if the numerical results are not truly global, i.e., ergodic on the phase space, the  $K$  dependence can be much stronger, as found in the previous results for local diffusion [6]. We can also fit our scalings to the power-law scaling of the theory in [12], since there is an adjustable parameter in that theory that in effect determines the power.

#### IV. CONCLUSIONS AND DISCUSSION

Arnold diffusion has been studied in  $N$  weakly coupled standard maps in which  $m$  phases  $m \leq N$  appear in the coupling term. The coupled system was symplectic (derived from a generating function). The rate of diffusion in the  $N$ -dimensional phase space was compared with previous results obtained for area preserving but nonsymplectic (for  $m < N$ ) coupled maps. There appears to be little difference in the diffusion rates of the symplectic and nonsymplectic systems. The diffusion rates for relatively large  $K$  can be normalized by dividing by  $N^{1/2}$  such that  $N$  does not explicitly appear. When this is done, the spread of the action  $\Delta I_{\text{rms}}$ , after a given number of mapping steps  $n$ , and fixing the mapping parameter  $K$  and the coupling parameter  $\mu$ , lies on separate universal curves of  $\Delta I_{\text{rms}}(m)$  for  $m < N$  and for  $m = N$  (see Fig. 2). For smaller  $K$  values the  $N$  scaling cancels, as can be explained, theoretically, from phase space arguments.

In previous work [6] an analytic formula to predict the

diffusion rate was developed, but not fully tested. The theory has now been compared to the numerical results for  $K = 0.8, 0.4,$  and  $0.3$ , shown in Figs. 2, 3, and 5, respectively. Because the phase space areas of the various types of orbits are not well known for the  $K = 0.4$  and  $0.3$  cases the theoretical results are bracketed, as described in the text. The results indicate reasonable agreement between theory and numerics but the numerical results have a somewhat steeper dependence on  $K$  than the theory.

Because the numerical results are very difficult to obtain for small  $K$ , the scaling of  $\Delta I_{\text{rms}}$  with  $K$ , extended to small  $K$  was obtained from the theory. The results, in Fig. 5, indicate a slow power-law decrease in diffusion rate with  $K$ ,  $\Delta I_{\text{rms}} \propto K^{0.25}$ . This dependence gives a value of  $D \propto \mu^2 K^{1/2}$  which is much weaker than that found in other studies [11,12]. Although the weak dependence is qualitatively understood in terms of the scaling of the dominant terms in the theoretical expression, it is not clear if this behavior is generic, depends on special properties of the coupling term, or results from the ergodic assumption which may not be satisfied in numerical studies.

#### ACKNOWLEDGMENTS

The work was partially supported by National Science Foundation Grant No. PHY-9505621. Many of the numerical calculations were done using a program of Dr. B. Wood. H. Lee performed initial calculations of local diffusion. Conversations with Professor M. A. Lieberman have been helpful.

- 
- [1] V. I. Arnold, Russ. Math. Surv. **18**, 85 (1964).
  - [2] B. V. Chirikov, Phys. Rep. **52**, 263 (1979).
  - [3] J. L. Tennyson, M. A. Lieberman, and A. J. Lichtenberg, in *Nonlinear Dynamics and the Beam-Beam Interaction*, edited by M. Month and J. C. Herrera, AIP Conf. Proc. No. **57** (AIP, New York, 1979), p. 272.
  - [4] A. J. Lichtenberg and M. A. Lieberman, *Regular and Stochastic Motion* (Springer-Verlag, New York, 1983).
  - [5] B. P. Wood, A. J. Lichtenberg, and M. A. Lieberman, Phys. Rev. A **42**, 5885 (1990).
  - [6] B. P. Wood, A. J. Lichtenberg, and M. A. Lieberman, Physica D **71**, 132 (1994).
  - [7] N. N. Nekhoroshev, Russ. Math. Surv. **32**, 6 (1977).
  - [8] A. Giorgilli, Ann. Inst. Henri Poincaré Phys. Theor. **48**, 423 (1988).
  - [9] P. Lochak, Phys. Lett. A **143**, 39 (1990).
  - [10] B. V. Chirikov, J. Ford, and F. Vivaldi, in Ref. [3], p. 323.
  - [11] T. Konishi and K. Kaneko, J. Phys. A **23**, 1715 (1990).
  - [12] B. V. Chirikov and V. V. Vecheslavov, J. Stat. Phys. **71**, 243 (1993).
  - [13] H. Kook and J. D. Meiss, Physica D **35**, 65 (1989).
  - [14] A. J. Lichtenberg and B. P. Wood, Phys. Rev. A **39**, 2153 (1989).